

SUPPLEMENTAL MATERIAL

Muscle LIM Protein Force-Sensing Mediates Sarcomeric Biomechanical Signaling in Human Familial Hypertrophic Cardiomyopathy

Running title: *Riaz et. al.; Biomechanical Signaling in HCM*

Muhammad Riaz, PhD^{1-4, *}, Jinkyu Park, PhD^{1-4, *}, Lorenzo R. Sewanan, MD, PhD^{5, *}, Yongming Ren, PhD¹⁻⁴, Jonas Schwan, PhD⁵, Subhash K. Das, PhD¹⁻⁴, Pawel T. Pomianowski, MD⁶, Yan Huang, PhD¹⁻⁴, Matthew W. Ellis, BS^{1,2,4,7}, Jiesi Luo, PhD¹⁻⁴, Juli Liu, PhD⁸, Loujin Song, PhD^{9,10}, I-Ping Chen, DDS, PhD¹¹, Caihong Qiu, PhD², Masayuki Yazawa, PhD^{9,10}, George Tellides, MD, PhD¹², John Hwa, MD, PhD^{1,4}, Lawrence H. Young, MD^{1,7}, Lei Yang, PhD⁸, Charles C. Marboe, MD¹³, Daniel L. Jacoby, MD¹, Stuart G. Campbell, PhD^{5,7}, and Yibing Qyang, PhD^{1-4, #}

¹Yale Cardiovascular Research Center, Section of Cardiovascular Medicine, Department of Internal Medicine, Yale School of Medicine, New Haven, CT, USA

²Yale Stem Cell Center, New Haven, CT, USA

³Department of Pathology, Yale School of Medicine, New Haven, CT, USA

⁴Vascular Biology and Therapeutics Program, Yale University School of Medicine, New Haven, CT, USA

⁵Department of Biomedical Engineering, Yale University, New Haven, CT, USA

⁶Department of Genetics, Yale University, New Haven, CT, USA

⁷Department of Cellular and Molecular Physiology, Yale University, New Haven, CT, USA

⁸Department of Pediatrics, Anatomy and Cell Biology, Indiana University, Indianapolis, IN, USA

⁹Department of Rehabilitation and Regenerative Medicine, Columbia Stem Cell Initiative, Columbia University, New York, NY, USA

¹⁰Department of Molecular Pharmacology and Therapeutics, Columbia University, New York, NY, USA

¹¹Department of Oral Health and Diagnostic Sciences, University of Connecticut Health, Farmington, CT, USA

¹²Department of Surgery, Yale University, New Haven, CT, USA

¹³Department of Pathology and Cell Biology, Columbia University, New York, NY, USA

*These authors contributed equally: Muhammad Riaz, Jinkyu Park, Lorenzo R. Sewanan.

Address for Correspondence:

Yibing Qyang, PhD

Yale University School of Medicine

Suite 773A, 300 George Street

New Haven, CT 06511

Phone: 1-203-737-6354

Email: yibing.qyang@yale.edu

Expanded Methods

Animal use for mouse embryonic fibroblast (MEF) isolation

Pregnant CF1 mice on embryonic day (ED) 12.5-13.5 were purchased from Charles River Laboratories (www.criver.com) for the derivation of mouse embryonic fibroblasts (MEFs) for maintenance of induced pluripotent stem cells (iPSCs) under the approval of the Institutional Animal Care and Use Committee (IACUC) of the Yale School of Medicine. Dissected and minced embryos were digested with 0.05% Trypsin-EDTA (Gibco; 25-300-054) to get single cells and were cultured in MEF medium containing DMEM (Gibco; 11965-092), 10% fetal bovine serum (FBS) (Gibco; 10082-147), 1% non-essential amino acid (v/v; Gibco; 11140050), 1% PenStrep (v/v; Gibco; 15070063), and 2 mM L-Glutamine (Gibco; 25030149). MEFs were expanded to passage 4 or 5, irradiated at 50 grays to induce mitotic arrest, and used as a feeder layer to support iPSC self-renewal. All animal care was in compliance with the NIH Guidelines for the Care and Use of Laboratory Animals.

Patient-specific iPSC generation

Generation of iPSCs from patients was conducted as previously described⁴⁶. Briefly, PBMCs were isolated from the proband family members and cultured in Roswell park memorial institute (RPMI) 1640 (Gibco; 11875093) for 5 days on anti-CD3 antibody-coated plates (BD Pharmingen, 555336). CytoTune™-iPSC 2.0 Sendai Reprogramming Kit (ThermoFisher Scientific; A16517) was used to reprogram PBMCs into iPSCs. The kit included three vector preparations: polycistronic KLF4–OCT3/4–SOX2, c-MYC, and KLF4. Each Sendai preparation containing 3×10^6 cell infection unit (CIU) particles was thoroughly mixed with 1 mL of pre-warmed RPMI-1640 medium at 37°C. PBMCs were collected into a 15 mL conical and centrifuged at 200 g for 5 minutes. The medium was then aspirated and replaced with 1 mL medium containing virus particles followed by cell seeding into each well. Twenty-four hours after viral transduction, infected PBMCs were harvested using 0.05% trypsin/EDTA and plated onto a mitotically arrested MEF feeder layer with human iPSC medium described above. The medium was next changed every day. About three weeks later, iPSC colonies started to emerge. Multiple colonies per line were picked up and expanded on MEF feeder layers for subsequent characterizations

and cardiac differentiation. iPSC lines with comparable passage numbers across genotypes were used in experiments. MYH7-R663H iPSC line⁷ was obtained from Dr. Joseph C. Wu at the Stanford Cardiovascular Institute. Additionally, MYBPC3-R943x and MYBPC3-V321M iPSC lines^{41, 42} were provided by Dr. Wu funded by NHLBI BhiPSC-CVD 75N9202D00019.

Cardiac differentiation

Cardiac differentiation was performed as previously described²⁶. Briefly, iPSCs were seeded on MEF and grew until 70-80% confluency (~4-5 day). They were then dissociated from culture dishes using 1 mg/mL of Dispase II (Gibco; 17105041) for 7-9 minutes. The iPSCs were further mechanically dissociated using a 5 mL pipette, collected in a 15 mL falcon tube, and spun down at 200 rpm for 4 minutes. The top supernatant was discarded to deplete the MEF cells. The pellet of iPSCs was then resuspended in mTeSR™ 1 (Stemcell Technologies; 05850) containing 5 µM ROCK inhibitor (Y-27632 dihydrochloride; Tocris Bioscience; 1244) and re-plated 1:1.5 on Growth Factor Reduced (GFR) Matrigel-coated (Corning; 1:60 diluted in DMEM/F12) plates. After reaching 80-95% confluency (in about ~1-2 days), cardiac differentiation was initiated. On day 0, 20 µM of CHIR99021 (Selleckchem; S2924) was added into a medium containing three volumes of RPMI-1640 supplemented with 1% B27 minus insulin (Gibco; A18956-01) and one volume of mTeSR™ 1. On day 1, the medium was changed to fresh RPMI-1640 containing 1% B27 minus insulin without additional factors. On day 3, the medium was changed to fresh RPMI-1640 containing 1% B27 minus insulin with the addition of 5 µM IWP-4 (Stemgent Reprocell; 04-0036), a Wnt inhibitor. On day 5, the medium was changed again to fresh RPMI-1640 containing 1% B27 minus insulin without additional factors and replenished every other day. Beating cardiomyocytes (CMs) were typically observed between day 9-11. On day 11, the medium was replaced with RPMI-1640 containing 1% B27 with insulin (Gibco; 17504044). Noncardiomyocytes could be eliminated starting from day 13 by treating the culture with 4 mM lactate (Sigma-Aldrich; L7022) in DMEM without glucose (Gibco; 11966025) for 4 days. Enriched CMs were then recovered for an additional 2 days in RPMI-1640 containing 1% B27 with insulin. On day 19, CMs were dissociated into clusters using a mixture of 10 µg/mL Collagenase A

(Roche;10103586001) and B (Roche; 11088807001) for 30 minutes at 37°C. They were further dissociated into single cells using Accutase™ (Sigma-Aldrich; A6964) for an additional 10 minutes at 37°C. Single CMs were then plated onto fibronectin-coated tissue culture plates using RPMI-1640 containing 1% B27 with insulin and 10% fetal bovine serum (FBS, Gibco; 10082-147) for 24 hours. On day 20-35, the culture medium was refreshed with RPMI-1640 containing 1% B27 with insulin every other day until harvesting for characterizations with immunofluorescence, mRNA expression, and protein analyses. CMs derived from proband iPSC clones one and two showed similar levels of expression of HCM markers, *ANF* and *BNP*, and were larger than iPSC-CMs derived from his parents. Proband iPSC clone one was used in studies involving his parents and clone two was used in the rest of studies.

Immunofluorescence staining of iPSC-CMs in cell culture

On day 35, CMs were fixed with 4% paraformaldehyde (ProSciTech; EMS15714) for 12 minutes at room temperature, washed with Dulbeccos Phosphate Buffered Saline (DPBS, Sigma-Aldrich; D8537), and permeabilized with 0.1% Triton X-100 (AmericanBio, Inc; 9002-93-1) for 20 minutes at room temperature. iPSC-CMs were then stained for cTnT, α -actinin, MLP, calcineurin, green fluorescent protein (GFP), and NFATc4 proteins. The antibodies used for immunofluorescence included mouse anti-cTnT (ThermoFisher Scientific; MS-295-P0), rabbit anti-cTnT (Abcam; ab92546), rabbit anti-GFP (ThermoFisher Scientific; A-11122), rabbit anti-MLP (Abcam; ab172952), mouse anti- α -actinin (Cell Signaling Technology; 3134), rabbit anti- α -actinin (Abcam; ab137346), rabbit anti-calcineurin (Abcam; ab109412), mouse anti-calcineurin (BD Transduction Laboratories; 610259), goat anti-NFATc4 (Santa Cruz Biotechnology; sc-1153), mouse anti-NFATc4 (Santa Cruz Biotechnology; sc-271597). An inverted fluorescent microscope (Leica; DM-IRB) was used for imaging iPSC-CMs cultured on tissue culture plastics. Confocal fluorescent microscope (Leica; Multiphoton Microscope TCS SP8 MP) was used to image immunostained heart tissue. ImageJ was used to measure cell area and mean fluorescence pixels (intensity) of whole-cell GFP and nuclear NFATc4. Mean fluorescence intensity (MFI) of GFP or nuclear NFATc4 per cell (grayscale) was corrected

by subtracting the background signals derived from the average of fluorescence pixels from three distinct non-cell areas.

Gene expression analysis

Total RNA was isolated from day 35 iPSC-CMs using TRIzol™ kit (ThermoFisher Scientific; 12183555) and cDNA synthesis was carried out using the iScript™ cDNA synthesis kit (Bio-Rad Laboratories; 1708891) according to manufacturer's protocols. Briefly, 3.5 ng of cDNA was included per reaction of 15 µL for each sample using gene specific primers (see Table S3). Quantitative PCR was carried using IQ™ SYBR Green Supermix (Bio-Rad Laboratories; 1708882) on CFX96 Optical Reaction Module for Real-Time System (Bio-Rad Laboratories; 1845096). All experiments were conducted in triplicate. Cycle threshold (CT) was calculated under default settings with real-time sequence detection software (Bio-Rad Laboratories; 1845001). Analysis was performed using Livak *et al.* 2001 $\Delta\Delta$ CT method and fold change was presented⁴⁷.

Western blot analysis and immunoprecipitation

Proteins were extracted by directly lysing day 35 iPSC-CMs in cell culture wells with M-PER mammalian protein extraction reagent (ThermoFisher Scientific; 78501) supplemented with cOmplete™ Protease Inhibitor Cocktail (Roche; C756U27) and Phosphatase Inhibitor Cocktail 2 (Sigma-Aldrich; P5726) followed by sonication. Samples containing 30-50 µg total protein were loaded on SDS-PAGE and western blotting were carried out with the PVDF membranes. The membranes were incubated with specific primary antibodies followed by horseradish peroxidase (HRP) conjugated secondary antibodies. The immunoblots were incubated with SuperSignal™ West Pico PLUS Chemiluminescent Substrate (ThermoFisher Scientific; 34579) and protein bands were visualized with the BOX Chemi XX6, Gel Documentation and ECL Detection System. The primary antibodies used included rabbit anti-MLP (Abcam; ab42504), mouse anti-phospholamban (PLB) monoclonal antibody (ThermoFisher Scientific; MA3-922), rabbit anti-P-PLB S16-P (Badrilla; A010-12AP), mouse anti-SERCA2A (Thermo Scientific; 2A7-A1), rat anti-calcineurin A (R & D Systems; MAB2839), and mouse anti- α -actinin (Sigma-Aldrich; A7811). HRP-conjugated goat anti-rabbit IgG (Vector Laboratories Inc; PI-1000),

horse anti-mouse IgG (Vector Laboratories Inc; PI-2000), or goat anti-rat IgG (R & D Systems; HAF005) secondary antibodies were used for the appropriate primary antibodies.

For immunoprecipitation experiment, day 35 iPSC-CMs were scraped into the lysis buffer (1% NP-40, 0.25% deoxycholate, 2 mM EGTA, 1 mM EDTA, 50 mM Tris-HCl) containing protease and phosphatase inhibitor cocktail. Cells were lysed by passing through the syringe with 20G needle for 10 times. Protein lysates were then incubated on ice for 20 minutes followed by centrifugation at 10,000 rpm at 4°C. Supernatants were transferred to new ice-cold tubes and the total proteins were quantified using the protein assay kit-1 (Bio-Rad Laboratories; 5000001). 100-500 µg total protein was used for each immunoprecipitation using A/G plus-agarose beads (Santa Cruz Biotechnology; SC-2003) as per vendor's instruction.

Calcium imaging

On day 30 of differentiation, iPSC-CMs were dissociated with Accutase for 7-10 minutes. Cells were then seeded onto a coverslip coated with 0.1% gelatin (Sigma-Aldrich; ES-006-B) and cultured in DMEM medium containing 10% FBS overnight. Medium was changed to RPMI-B27 medium the next day. On day 35, iPSC-CMs were loaded with 10 µM Fura-2 acetoxymethyl ester (Molecular Probe; F1221) and 0.1% pluronic F-127 (Sigma-Aldrich; P2443) in Tyrode solution (NaCl 148 mM, KCl 5 mM, CaCl₂ 1.8 mM, MgCl₂ 1 mM, glucose 10 mM, HEPES 10 mM, at pH 7.4) for 20 minutes at room temperature. Non-incorporated dye was washed away with Tyrode solution for 15 minutes. CMs were paced at 1Hz, and fluorescence intensities at 510 nm with 340 nm and 380 nm excitation were collected at a rate of 10 kHz using a photomultiplier tube (PMT). Data were analyzed in a custom MATLAB program. Cytosolic Ca²⁺ was measured by a ratio of fluorescence intensity at 340 nm and 380 nm (F₃₄₀/F₃₈₀).

Engineered heart tissue (EHT) generation and cell seeding

EHTs were generated by seeding iPSC-CMs into decellularized laser-cut porcine myocardium as described in our previous report²². Briefly, thinly sliced porcine myocardium was laser-cut and decellularized by incubating the tissues in a cell lysis

buffer (10 mM Tris, 0.1% weight/volume EDTA, pH 7.4) for 2 hours followed by a 40-minute incubation in sodium dodecyl sulfate (0.5% weight/volume in DPBS) with gentle agitation (35 rpm on an incubated shaker) at room temperature. Tissues were washed three times in DPBS and incubated in DMEM containing 10% FBS and 1x PenStrep for 24 hours in a cell culture incubator. On day 14 of cardiac differentiation, iPSC-CMs were detached with Accutase for 20 minutes at 37°C. Mechanical disruption was applied every 5 minutes to get a homogenous suspension of cells. The cells were washed with MEF medium, DPBS, and MEF medium, respectively, and spun down at 1,000 rpm after each washing. Finally, cells were resuspended in MEF medium containing 5 μ M ROCK inhibitor, and a cell suspension of 10-million cells per mL was made. 100 μ L of cell suspension was seeded into an already assembled EHT cassette (1 million cells per EHT).

Mechanical and functional testing of EHTs

To investigate contractile mechanics, EHTs were measured in a custom muscle mechanical setup at day 30 post cardiac differentiation²². Clips holding the EHT were gently ejected from the frame and picked up by motorized micromanipulators with claw-like extensions, leaving the muscle suspended between an anchoring attachment claw on one end and a force transducer mounted to a second claw on the other end (Figure 1G cartoon). The EHT was immersed in a temperature-controlled perfusion bath equipped with electrodes for field stimulus. Throughout the measurements, scaffolds were perfused with freshly oxygenated Tyrode's solution (NaCl 140 mM, KCl 5.4 mM, MgCl₂ 1 mM, HEPES 25 mM, glucose 10 mM, and CaCl₂ 1.8 mM; pH adjusted to 7.35). All measurements were performed at 36°C with 1Hz field stimulus (100 mA constant current, 10 ms pulse width). After preconditioning at different lengths and frequencies, EHT mechanics were recorded at 10% stretch (6.6 mm). Twenty twitches were recorded, averaged, and used to quantify the peak force, time to peak force (TTP), and time from peak force to 50% relaxation (RT50), as previously described²².

Cloning and site-directed mutagenesis to generate MLP-W4R and HA-tagged MLP-WT and MLP-W4R

MLP cDNA was purchased from OriGene (RC203241). Primers containing Sall and AgeI restriction sites (see Table S3) were used to amplify MLP coding region, and the PCR product was cloned into sin18-PGK-MCS-IRES-GFP lentivirus vector. Validation of this plasmid was done through sequencing by the Keck DNA Sequencing - Yale School of Medicine, Yale University. MLP-W4R missense mutation was introduced using the QuickChange Lightning Site-Directed Mutagenesis Kit (Agilent; 210518). Mutagenesis was confirmed by Sanger sequencing. HA-tag sequence was introduced at the N-terminus of MLP-WT or MLP-W4R using a forward primer linked with the HA-tag sequence. HA-tagged MLP and MLP-W4R cDNAs were confirmed by Sanger sequencing and then cloned into lentiviral vector.

Lentivirus production and qPCR-based viral titration

Briefly, Sin18-PGK-IRES-GFP, and Sin18-PGK-HA-MLP-IRES-GFP or Sin18-PGK-HA-MLP-W4R-IRES-GFP plasmid was co-transfected in HEK-293T cells with two additional lentiviral packaging plasmids that encode VSVG and gag/pol. Conditioned medium containing lentiviruses was collected 48 and 72 hours post transfection. Lentivirus particles were quantified using Lenti-X™ qRT-PCR Titration Kit (TAKARA Bio Clontech; 631236) as per manufacture's instruction. More than 70% confluent iPSC-CMs were infected with lentivirus on day 21 or day 22 of cardiac differentiation. Medium was refreshed 24 hours post infection. Infected iPSC-CMs were then cultured to day 35 with a medium change of every other day before harvesting for analyses.

Clustered Regularly Interspaced Short Palindromic Repeats (CRISPR)-mediated gene editing for MYH7-R723C correction

Custom single guide RNA (gRNA) targeting the MYH7-R723C point mutation was designed using a web-based *in silico* CRISPR Design Tool (<http://crispr.mit.edu/>)⁴⁸. The gRNA designated with the highest score was cloned into a plasmid that expresses *Streptococcus pyogenes*-derived endonuclease: CRISPR associated protein 9 (Cas9). The plasmid consists of both a gRNA scaffold backbone and a Cas9 encoding cassette. The cloned gRNA was verified using the Sanger sequencing. A donor DNA template of 901 bases was synthesized (Quintara Bioscience), cloned into a pUC19 vector through

direct end ligation, and transfected into iPSCs to facilitate homology directed repair (HDR) and correction of the mutant base to the wild-type sequence. The BamHI restriction site was introduced into the donor template DNA via silent base substitutions to facilitate subsequent screening for iPSC clones with successful HDR through PCR amplification of the target region followed by restriction enzyme digestion. The protospacer adjacent motif (PAM) sequence of the gRNA in the donor template DNA was eliminated through a silent base substitution to minimize cleavage of the donor template DNA or recleavage of the corrected target sequence by Cas9. iPSCs grown on a GFR-Matrigel-coated 6-well plate in mTeSR™ 1 medium (40-50% confluency) were co-transfected with a mixture of 1.5 µg gRNA-Cas9 plasmid, 1.5 µg donor plasmid, and 0.5 µg GFP expressing plasmid using Lipofectamine™ LTX Reagent with PLUS (Invitrogen;15338100). 24 hours after transfection, medium containing the transfection mixture was replaced with fresh medium and cells were cultured for an additional 48 hours. Transfected cells were then dissociated into single cells using Accutase followed by fluorescence-activated cell sorting (FACS) based on GFP expression. About 5-10 thousand sorted cells were plated onto GFR-Matrigel-coated 10-cm tissue culture dishes and cultured in the hypoxia incubator (5% O₂) for 48 hours without medium change. Subsequently, medium was refreshed every other day until the emergence of distinct clones about two weeks after plating. Individual clones with distinct boundaries were picked up for HDR analysis. Briefly, one-third of each clone was transferred into a well of a GFR-Matrigel-coated 48-well plate for expansion, and two-thirds of each clone was transferred to a 0.2 mL PCR tube that contains 15 µL DirectPCR Lysis Reagent (Viagen Biotech; 301-C) supplemented with 10% proteinase K (Qiagen, Inc; 19131) for cell lysis and DNA extraction. Complete cell lysis was achieved by incubating cells at 56°C for 15 hours, and proteinase K was next inactivated at 95°C for 15 minutes. Cell lysate was directly used as the genomic DNA template for PCR reaction to amplify a 701 bp amplicon flanking the point mutation and the gRNA PAM sequence. The 701 bp PCR products from all clones were then digested with BamHI for two hours at 37°C followed by confirmation of restriction digestion on 2% agarose gel. Clones showing the right restriction digestion pattern were further confirmed for the gene correction by Sanger sequencing. Two iPSC clones showing correction for the R723C

mutant allele were selected for karyotyping, potential off-target sequencing, and cardiac differentiation.

Transcription activator-like effector nuclease (TALEN)-mediated gene editing for MLP-W4R correction

The heterozygous MLP-W4R missense mutation was corrected using the TALEN-mediated genome editing technology. The left and right TALEN flanking the MLP-W4R missense mutation were synthesized by the Life technologies, Invitrogen. The TALENs were initially cloned into the Gateway adapted vector and then subcloned into a vector in which the expression of TALEN proteins was driven by the pEF1 α promoter that is highly active in iPSCs. A 135 bp anti-sense single-stranded oligodeoxynucleotides (ssODN; antisense) with MLP-W4R missense sequence corrected to wild type was used as the donor template. The MfeI restriction site (CAATTG) was introduced into the donor template via silent base substitutions to facilitate subsequent screening for iPSC clones with HDR. As to TALEN transfection, iPSCs were seeded onto a Geltrex (Gibco™; A1413302) coated 6-well tissue culture plate in Essential 8™ medium (Life Technologies; A1517001) so that the cell density would reach 40%-50% the next day. Lipofectamine LTX and Plus reagents were used to accomplish transfection in iPSCs. DNA cocktail containing left and right TALEN encoding plasmids, ssODN, and a GFP expressing plasmid (1.5:1.5: 0.5: 0.1, unit as μ g) was made in 100 μ L E8 medium. The transfection cocktail was made by adding 7.5 μ L transfection reagents into 100 μ L of E8 medium. After incubating both cocktails at room temperature for 5 minutes, the transfection cocktail was added to the DNA cocktail, followed by thorough mixing with a micropipette and an additional incubation for 30 minutes. A transfection in the absence of GFP was also prepared for an iPSC well as a negative control for FACS. Before transfection, old medium in iPSCs was replaced with fresh PenStrep-free E8 medium containing 5 μ M ROCK inhibitor. TALEN transfection mixture was added dropwise to the corresponding wells, and the plate was then placed into the incubator for 45 minutes. Medium containing transfection mixtures was then removed and replenished with fresh E8 medium with Pen-Strep. The medium was refreshed the next day. iPSCs were dissociated with Accutase into single cells for FACS based on GFP expression 48 hours after transfection. About 5-

10 thousand FACS sorted cells were seeded on the Geltrex coated 10 cm² tissue culture dish and cultured in the hypoxia incubator (5% O₂) for 48 hours without medium change. Subsequently, medium was changed daily until visibly iPSC colonies emerged in about 10 days. Individual clones with distinct boundaries were picked up for HDR analysis. Two clones with gene correction were selected for karyotyping and cardiac differentiation.

Computational modeling

A computational model of cooperative myofilament calcium-dependent activation with a three-state crossbridge cycle was employed to perform muscle mechanics simulations as previously described^{27, 28}. Generally, force transients (i.e. twitches) with model parameters for wild-type myosin (MYH7-WT) and mutant myosin (MYH7-R723C) were simulated using Ca²⁺ transients derived from the normal and mutant myosin cardiomyocytes. The calcium transients with properties closest to those of the average properties of those measured via Fura2 dye in the MYH7-WT and MYH7-R723C iPSC-CMs were digitized at a sampling rate of 1000 Hz and smoothed with a 20 ms moving average filter. The WT Ca²⁺ transient was normalized to have a diastolic value of 0.1 μM and a maximum value of 1.0 μM; the mutant MYH7-R723C Ca²⁺ transient was normalized such that its diastolic and systolic values maintained the average experiment relative change with respect to WT Ca²⁺. The relative properties of the MYH7-WT and MYH7-R723C Ca²⁺ transients were compared and found to be consistent with the relative changes of the measured MYH7-WT and MYH7-R723C non-normalized values. Twitches were chosen from amongst the measured data to be statistically representative in experimental properties for both MYH7-WT and MYH7-R723C iPSC-CMs. Force transients for both MYH7-WT and MYH7-R723C iPSC-CMs were then normalized to a maximum value of 1.0 for twitch kinetic analysis. The values of seven baseline model parameters were first determined by using the MYH7-WT Ca²⁺ transient and running the simulation at by varying those parameters to fit the MYH7-WT twitch by using a particle swarm stochastic optimization algorithm as previously implemented. Six constraints were placed on the model to fit the parameters for the MYH7-WT twitch, including the following: (1) root-mean-square-error of less than 0.1, (2) a maximum activation no lower than 0.10 and no higher than 0.50, (3) a calcium equilibrium constant between 0.005-1.000, (4) a

duty cycle between 0.1-0.8, (5) a blocked-closed equilibrium constant between 0.5-3000, and (6) a crossbridge scaling factor slower than that of the previous mouse fitting parameters. In this way, the seven parameters were constrained not only by the data but also by physiologically reasonable parameter ranges, comparable to experimental values and previous models. The particle swarm optimization was run at least three times using 100 particles for 100 iterations per particle to find the best solution. Once the baseline MYH7-WT parameters were found, parametric studies were conducted to find a change in a single parameter that would best recapitulate the MYH7-R723C twitch when fed the MYH7-R723C mutant Ca^{2+} transient. Once this parameter change was determined, sensitivity analyses were conducted to verify the robustness of the solution. Additional simulations were conducted using the MYH7-R723C Ca^{2+} transient with the WT model parameter set and the WT Ca^{2+} transient with the MYH7 mutant model parameter set in order to study contractile behaviors that could not be measured experimentally.

Luciferase assay for measuring NFAT transcriptional activity

NFAT transcriptional activities in iPSC-CMs were measured using a Dual-Glo® Luciferase Reporter Assay System (Promega) according to the manufacturer's instructions. Briefly, 25,000 of iPSC-CMs were seeded in each well of 48-well plate. The iPSC-CMs were transiently co-transfected at day 25 of cardiac differentiation with an NFAT-luciferase reporter plasmid (0.25 μg 9xNFAT-luciferase; a gift from Jeffery Molkentin; Addgene plasmid #51941; <http://n2t.net/addgene:51941>; RRID:Addgene_51941)⁴⁹ and a Renilla-luciferase plasmid (0.25 μg pLX313; a gift from William Hahn & David Root; Addgene plasmid #118016; <http://n2t.net/addgene:118016>; RRID:Addgene_118016)⁵⁰ that is regulated by the constitutively active EF-1 α promoter and served as an internal transfection control, using Lipofectamine™ 3000 Transfection Reagent (Invitrogen™; L3000008). Two days after transfection, cells were lysed with 1x Passive Lysis Buffer, followed by measurements of firefly luciferase activity with the Luciferase Assay Reagent II and then Renilla luciferase activity with the Stop & Glo® Reagent. NFAT-luciferase activities normalized by Renilla-luciferase activities in proband iPSC-CMs were determined, and fold-changes were calculated in relation to control iPSC-CMs. Regarding the NFAT-luciferase assay for DMSO vehicle control or mavacamten-

treated proband iPSC-CMs, 25,000 cells were incubated with DMSO or 0.5 μ M mavacamten on day 25 of cardiac differentiation for two days in 48-well plates. On day 27, DMSO or mavacamten was removed from cultures and NFAT-luciferase reporter and Renilla-luciferase plasmids were transfected for 6 hours, followed by replenishing the medium with fresh medium containing DMSO or 0.5 μ M mavacamten. NFAT-luciferase activities normalized by Renilla-luciferase activities were determined on day 29, and fold-changes were calculated in relation to DMSO-treated proband iPSC-CMs.

Evaluation of tissue fibrosis, sarcomere disarray, and Z-disc-localized MLP

Tissues derived from the proband septal myectomy were fixed in 10% neutral buffered formalin, embedded in paraffin, sectioned at 5 μ m thickness, and stained with Sirius Red by the histology core facility of Yale University. Left ventricular free wall tissues were obtained from a healthy young adult (18-year-old) died in a car accident, fixed in 10% neutral buffered formalin, embedded in paraffin, and used as the control in the studies. Tissue fibrosis was evaluated by Sirius Red staining. Immunofluorescence staining was performed for α -actinin, MLP, and 4',6-diamidino-2-phenylindole (DAPI) for DNA, and imaging was performed using Nikon Eclipse 80i upright fluorescent microscope to evaluate sarcomere disarray, myofiber misalignment, and Z-disc-localized MLP.

Drug treatments

Day 25 iPSC-CMs were treated with 0.5 μ M myosin ATPase inhibitor (MYK-461; also known as mavacamten), 0.5 μ g/mL calcineurin inhibitor (FK506), or DMSO vehicle control. After a 4-day drug treatment, iPSC-CMs were fixed with 4% paraformaldehyde (ProSciTech; EMS15714) for immunofluorescence staining. Additionally, iPSC-CMs were lysed with TRIzol™ reagent for messenger RNA (mRNA) analysis 24 hours after drug treatment or lysed with the M-PER Mammalian Protein Extraction Reagent for protein extraction 4 days after drug treatment. mRNA and protein expression levels of genes of interest were quantified with qRT-PCR and western blotting, respectively, as described in the sections above. For paired testing of EHTs treated with DMSO (vehicle) or 0.5 μ M mavacamten, Tyrode's solution containing DMSO or 0.5 μ M mavacamten was allowed to equilibrate until steady state (30 minutes) before mechanical testing as above²².

Supplemental Tables

Table S1. Clinical Characteristics of the proband patient and other family members.

HCM family members	Age (Year)	Mutation	Systolic/Diastolic function	Electrocardiogram (EKG)
Proband (III-2)	1.3	MLP-W4R; MYH7-R723C	Interventricular septum of 2.3 cm, posterior wall measured 0.4 cm, dynamic obstruction to left ventricular outflow with peak velocity of 4.7 m/sec.	Normal sinus rhythm, prominent Q-waves, left septal hypertrophy, left ventricular hypertrophy (LVH).
Proband's father (II-3)	36	MYH7-R723C	Normal size and function, interventricular septum of 1.3cm.	Normal sinus rhythm, normal EKG.
Paternal uncle (II-2)	40	MYH7-R723C	Normal size and function, interventricular septum of 1.1-1.4cm, benign, 1.4 cm inferior lateral hypertrophy.	Normal sinus rhythm, right ventricular hypertrophy (RVH), LVH.
Paternal cousin (III-1)	12	MYH7-R723C	Normal size and function.	Normal sinus rhythm, normal EKG.
Paternal grandmother (I-2)	59	MYH7-R723C	Left ventricular (LV) function estimated at 60%, mild diastolic dysfunction, ejection fraction (EF) 77%, interventricular septum of 1.1cm.	Normal sinus rhythm, left atrial abnormality, left atrial hypertrophy (LAH), prominent inferior Q-waves, hyperdynamic LV.
Proband's sister (III-3)	0.2	MLP-W4R	Normal size and function.	Normal sinus rhythm, normal EKG.
Proband's mother (II-4)	35	MLP-W4R	Normal size and function, interventricular septum of 0.8cm.	Normal sinus rhythm, normal EKG.
Maternal aunt (II-5)	33	MLP-W4R	Normal size and function.	Normal sinus rhythm, normal EKG.
Maternal grandmother (I-4)	55	MLP-W4R	Mild diastolic dysfunction.	Normal sinus rhythm, normal EKG.

Table S2. Myofilament model parameter sets. Baseline parameters were derived by fitting the computational model with WT calcium transient input to WT MYH7 twitch using a particle swarm stochastic optimization method^{27, 28, 37}. Hypothesis-driven changes in myosin parameters were used to fit R723C MYH7 data.

Parameters	Parameter description	WT MYH7 Fit (range)	R723C MYH7 Fit (range)	Units
k_{+Ca}	Rate of Ca ²⁺ binding to troponin	2.64 (2.62-2.66)	2.64 (2.62-2.66)	$\mu\text{M ms}^{-1}$
k_{-Ca}	Rate Ca ²⁺ dissociation from troponin	0.54 (0.52-0.56)	0.54 (0.52-0.56)	ms^{-1}
k_{+B}	Base rate for transition of Tm from nonpermissive to permissive	999.9 (899.9-1099.8)	999.9 (899.9-1099.8)	ms^{-1}
k_{-B}	Base rate for transition of Tm from permissive to nonpermissive	0.26 (0.25-0.28)	0.26 (0.25-0.28)	ms^{-1}
$\delta (f/[f+g])$	Crossbridge duty cycle	0.20	0.26	-
f	Crossbridge on rate	1.66 (1.50-1.83)	2.30 (2.24-2.49)	ms^{-1}
g	Crossbridge off rate	6.55 (5.90-7.20)	6.55 (5.90-7.20)	ms^{-1}
g_{xb}	ATP consuming transition rate	0.58 (0.55-0.61)	0.58 (0.55-0.61)	ms^{-1}
γ_b	Nearest neighbor RU cooperativity	4535.1 (4308.0-4762.0)	4535.1 (4308.0-4762.0)	-

#By definition, duty cycle δ is related to crossbridge on and off rates as follow: $\delta = \frac{f}{f+g}$

*Note that f (crossbridge on rate) is the only parameter that was allowed to change from WT to fit the R723C mutant, which corresponds to a duty cycle change as shown above (as discussed in methods).

Table S3. List of primers for qRT-PCR, genomic sequencing, cDNA subcloning, and target sequences for MLP and MYH7 gene editing.

Gene	Primer	Sequence 5'-3'
qRT-PCR primers		
<i>ACTA1</i>	fw-q	tcctcatcgggatggagtc
	rv-q	cagcgcggtgatctcttc
<i>ANF</i>	fw-q	caggatggacaggattggag
	rv-q	acaggagcctcttgcaagtct
<i>ANKRD1</i>	fw-q	tcaagaactgtgctgggaag
	rv-q	tagctatgagagaggcttg
<i>BNP</i>	fw-q	ttgggaggaagatggacc
	rv-q	tgtggaatcagaagcagggtg
<i>GAPDH</i>	fw-q	gaaggatgaaggtcggagtca
	rv-q	ttgaggatcaatgaaggggtc
<i>MCIP1</i>	fw-q	agtgggatggaacaagtg
	rv-q	gctgctgcaattcactt
Primers for genomic sequencing for MLP-W4R and MYH7-R723C mutations and for MLP cDNA subcloning		
MLP-genomic	fw	tggtctcagaccactgc
	rv	accacactatgagaaccact
MYH7-genomic	fw	caggatgaccctggaattc
	rv	cagaggagtcaatggaaaagagatg
Sall-MLP cDNA	fw	cgacgtcgacattactttctttccactgtgtgt
AgeI-MLP cDNA	rv	cgacaccggtgaggagatctgccccgcatcgc
Primers for site-directed mutagenesis of the heterozygous MLP-W4R mutation		
Primer with mutant nucleotide (in bold)		atgccatgcca acc ggggcggagg
Primer with wild-type nucleotide (in bold)		atgccatgcca act ggggcggagg
MLP-W4R left and right TALEN target sequences		
MLP-Right TALEN		nccagatagtcttcaagat
MLP-Left TALEN		nggctccacattttgcgcc
MYH7-R723C gRNA target sequence		
gRNA		actggttgatcaatgtcc

Table S4. Top ten potential candidate off-target genomic loci and PCR primers flanking the potential off-targets.

Off-target score*	Potential off-target genomic sequences (mismatch bases are in blue color)	Chromosomal location	PCR primers flanking potential genomic off-target
1.5	gctg tg tgatcaatgtcc	chr9:833593-833734	fw: gcagtcccactgtgccttc rv: gctgagtcagctggcttg
1.3	at ttt tgatcaatgtcc	chr8:84500374-84500573	fw: tatctatatatgttttaaatgaa rv: cagactggagacaaagacaag
1.1	actggt ct catcaatgtca	chr5:57445265-57445445	fw: tgattccctgtgaggcttg rv: cctgtaatttaaattgaacaac
0.8	gcag ttg agatcaatgtcc	chr1:22056555-22056766	fw: acttttagtttctcacacctc rv: ttttctaaaattgcaaaaaggg
0.8	c ct cctgtg ct caatgtcc	chr2:48963090-48963263	fw: gagcatggccatgcgcttg rv: atggatattgacagcccttg
0.8	act ctct tgatcaatgtcc	chr16:86945286-86945477	fw: ggtagccgcagaggaaaagc rv: caaatccattctcccacttc
0.8	ac at g ttg atcaatgtcc	chr16:13024909-13025135	fw: aataacatctgtcaaatgcaag rv: aacacagggtattctagaaac
0.7	gatg ttct gatcaatgt ct	chr6:74578219-74578429	fw: aggcaaaagctctggggaac rv: ctttagaaactaaaaataagcttc
0.7	at tgct tgatcaatgt ct	chr16:63889802-63890071	fw: aaaatgatggatagaggaaag rv: aaataaagaagcatcatgcttg
0.7	ac agct ctgatcaatgtca	chr17:27768969-27769156	fw: gaactgacctgaaggtttg rv: ggcaggtagcctgtgtttg

*Off-target scores were determined using the CRISPR design tool developed by the Massachusetts Institute of Technology⁴⁸ and was accessible via <http://crispr.mit.edu/>.

Figure S1

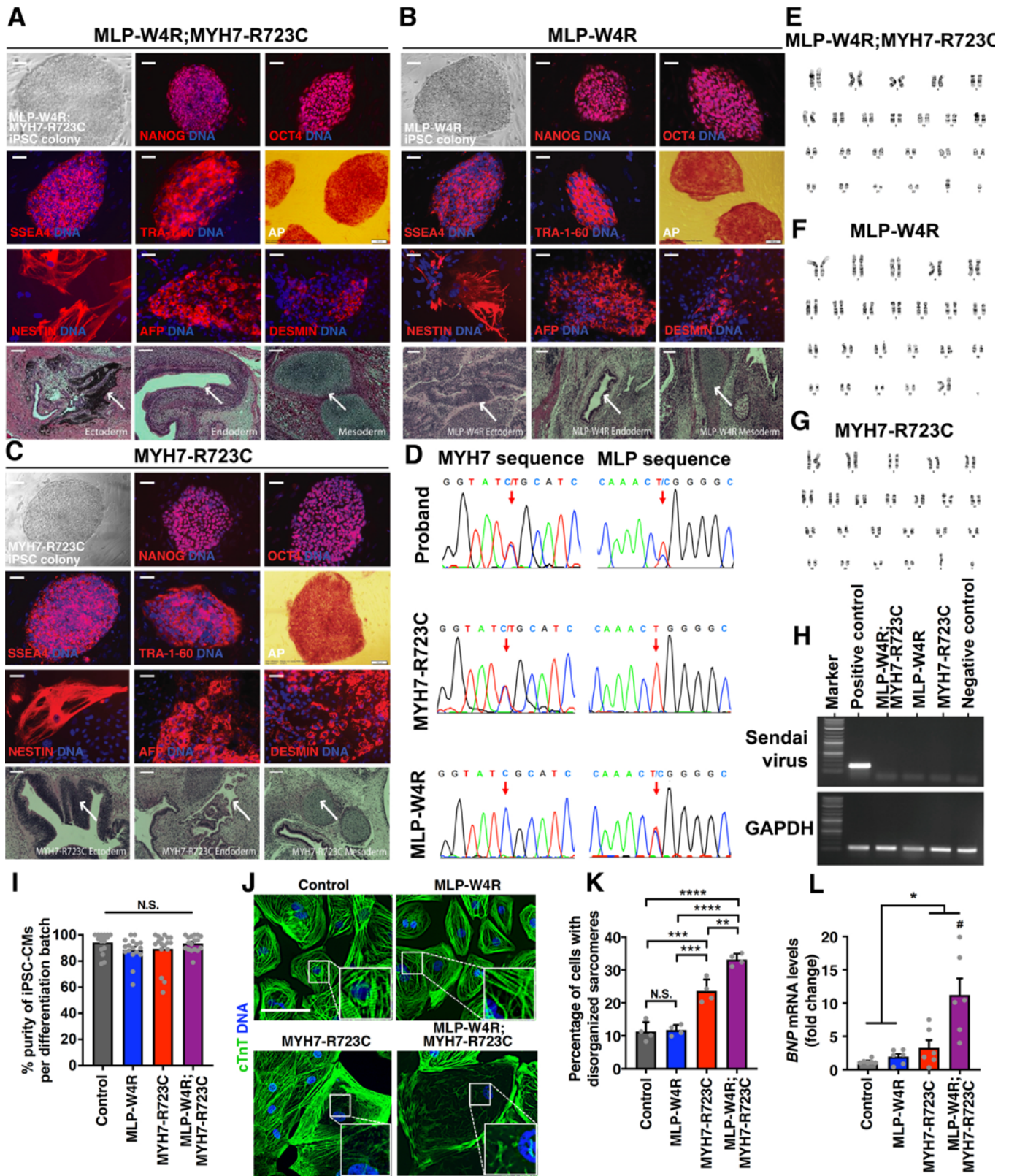


Figure S2

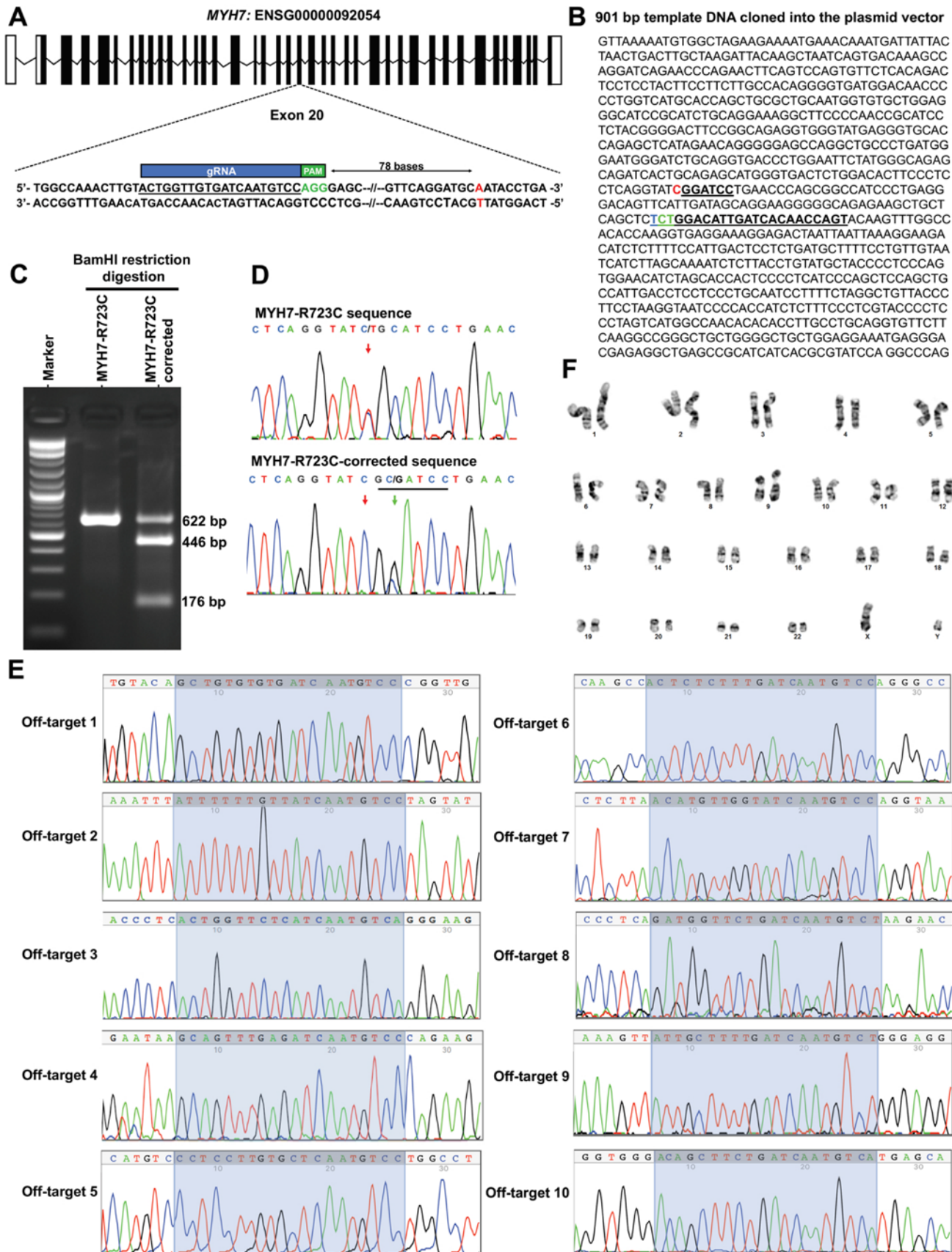


Figure S3

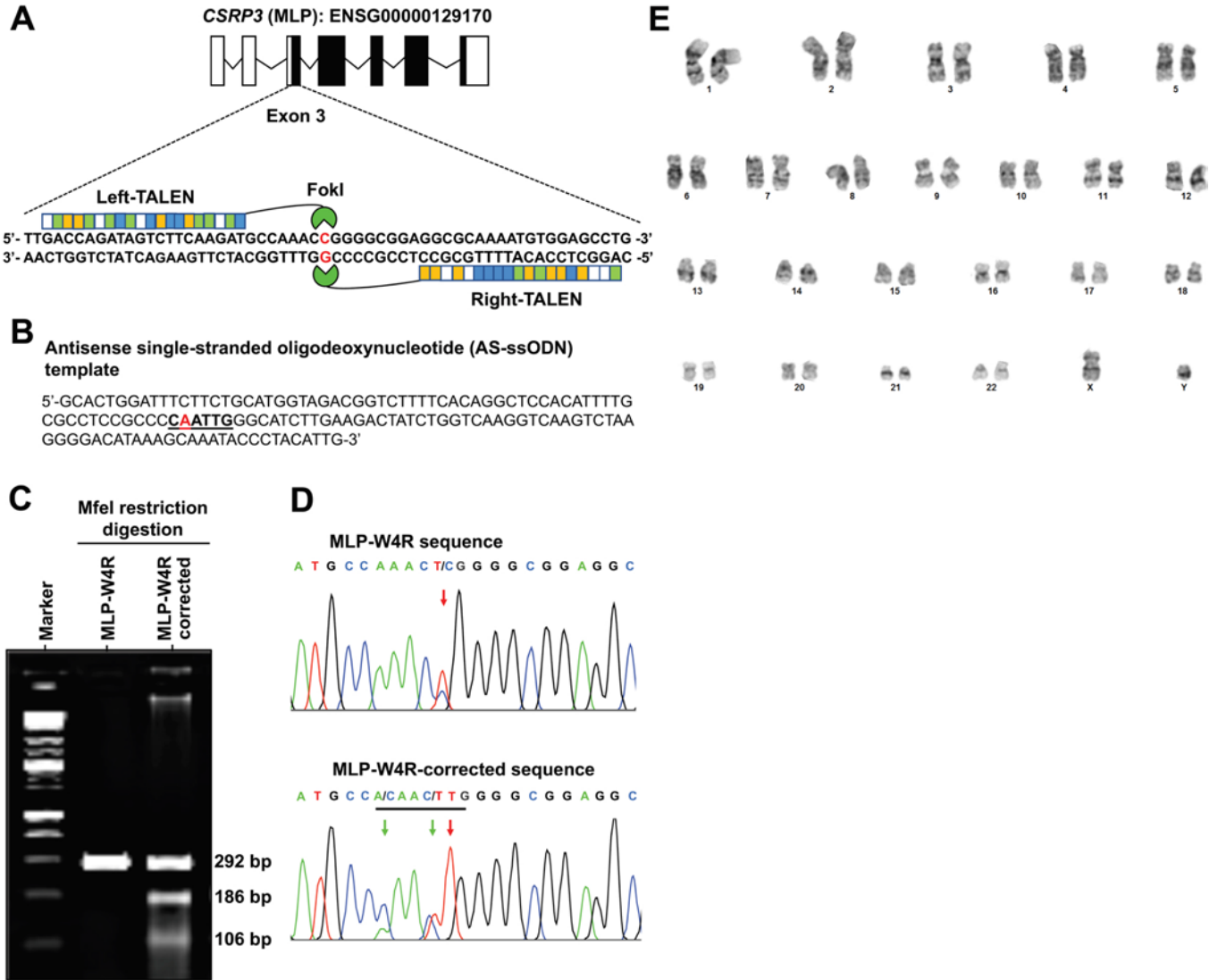


Figure S4

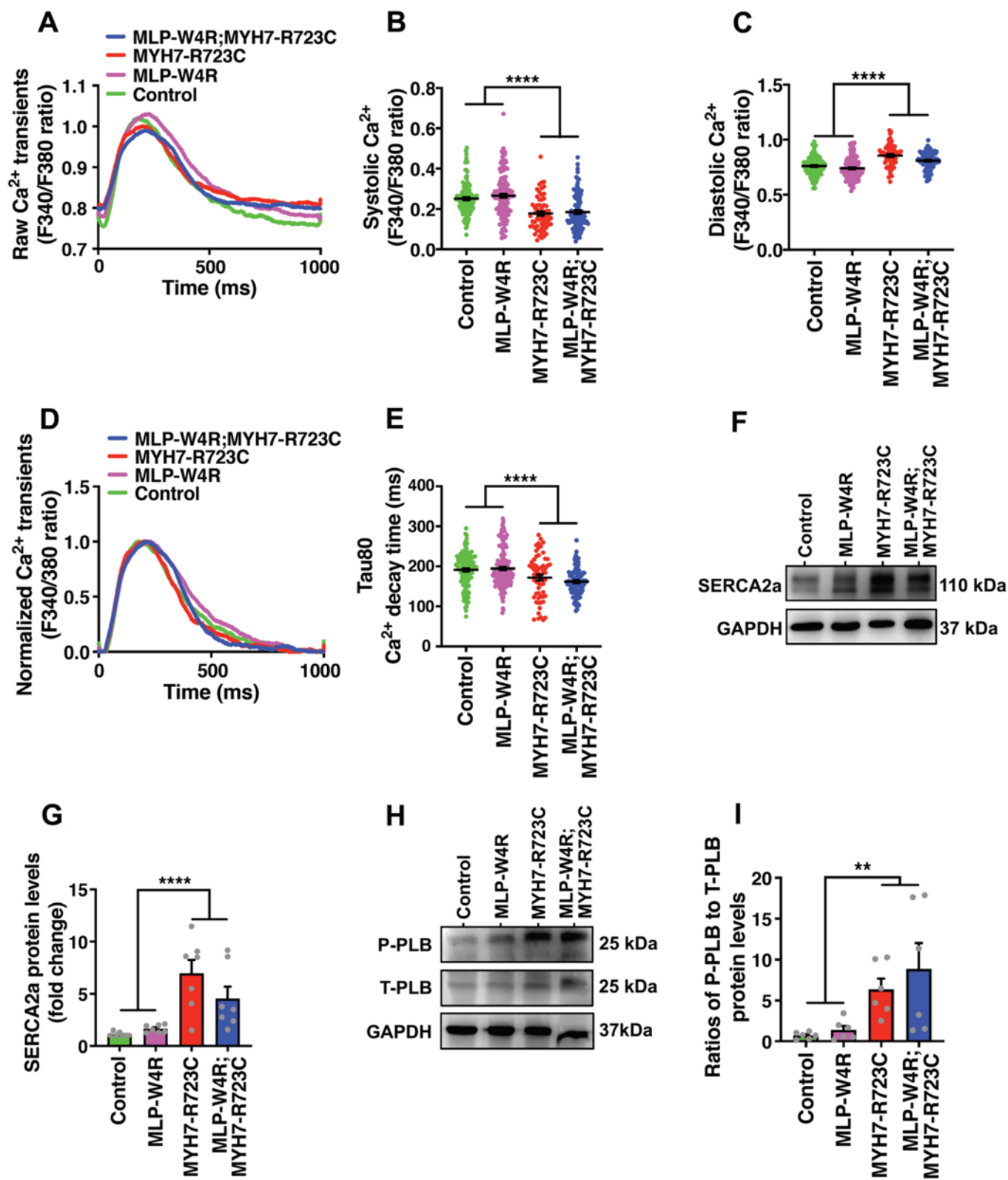
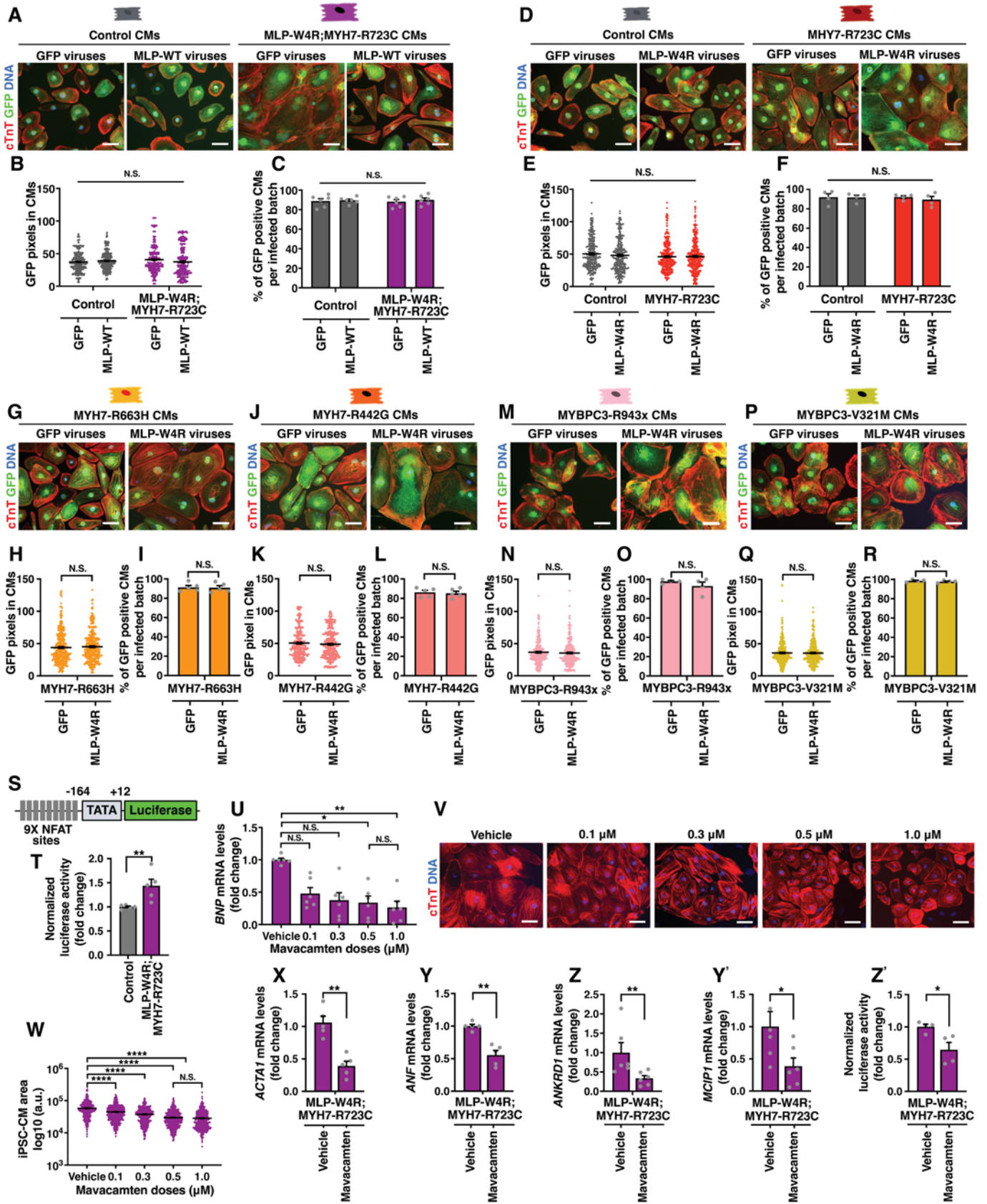


Figure S5



Supplemental Figure Legends

Figure S1. Characterization of MLP-W4R;MYH7-R723C, MLP-W4R, and MYH7-R723C iPSCs and iPSC-Derived Cardiomyocytes. Related to Figure 1.

A-C, A representative colony of iPSCs was derived by reprogramming the peripheral blood mononuclear cells (PBMCs) isolated from the blood of MLP-W4R;MYH7-R723C (**A**), MLP-W4R (**B**), and MYH7-R723C (**C**) individuals. Immunostaining was performed for the pluripotency markers (OCT4, NANOG, SSEA4, and TRA1-60) as well as an alkaline phosphatase (AP) staining of each of the stem cell colonies. *In vitro* embryoid body differentiation into the three germ layers was confirmed by the respective three germ layer markers, NESTIN, AFP and DESMIN. DNA was always counterstained by DAPI. Scale bar, 100 μ m (A-C). Teratoma assay with MLP-W4R;MYH7-R723C (**A**), MLP-W4R (**B**), and MYH7-R723C (**C**) iPSCs in immunodeficient mice were performed. All iPSC lines differentiated into three germ layers: ectoderm, endoderm and mesoderm, which were marked by the white arrows in the respective H & E images. Scale bar, 100 μ m. **D**, Confirmation of missense mutations in the proband, MLP-W4R, and MYH7-R723C iPSC-derived genomic DNA. The target DNA containing mutations was amplified using PCR primers flanking the mutations and confirmed by the Sanger sequencing. Primer sequences can be found in Table S3. **E-G**, Karyotyping of MLP-W4R;MYH7-R723C (**E**), MLP-W4R (**F**), and MYH7-R723C iPSCs (**G**). Chromosomes showed normal karyotypes. **H**, PCR-based detection of Sendai viruses in iPSCs of MLP-W4R;MYH7-R723C, MLP-W4R, and MYH7-R723C showed the absence of virus in all three iPSC lines. *GAPDH* PCR was used as DNA control. **I**, Purities of cardiomyocytes derived from control, MLP-W4R, MYH7-R723C, and MLP-W4R;MYH7-R723C proband iPSCs. The purities of cardiomyocytes were measured using cTnT immunostaining of day 35 control, MLP-W4R, MYH7-R723C, and MLP-W4R;MYH7-R723C iPSC-CMs (Figure 1H). ImageJ was used to quantify percent of cells positive for cTnT for each experimental group. Kruskal-Wallis with Dunn's multiple comparisons test was used for statistical evaluation and revealed no significant difference in iPSC-CMs purity ($H(3)=5.587$, $p=0.1335$). Data in the graph are presented as mean \pm S.E.M; $n=17$ independent cardiomyocyte differentiation batches; N.S.: not significant. **J**, Evaluation of sarcomere disarray in control, MLP-W4R,

MYH-R723C, and MLP-W4R;MYH7-R723C proband iPSC-CMs based on cTnT immunostaining of day 35 control, MLP-W4R, MYH7-R723C, and MLP-W4R;MYH7-R723C iPSC-CMs. DNA was counterstained by DAPI. Scale bar, 100 μ m. Representative images showing organized sarcomeres in control and MLP-W4R iPSC-CMs and disorganized punctate sarcomeres in MYH7-R723C and MLP-W4R;MYH7-R723C iPSC-CMs. **K**, Quantification of cells with disorganized sarcomeres in control, MLP-W4R, MYH7-R723C, and MLP-W4R;MYH7-R723C iPSC-CMs. Cells with disorganized sarcomeres were defined as having greater than 25% cell area with disorganized, punctate cTnT staining without appreciable striations. Two-way ANOVA with Tukey's multiple comparisons test was used for statistical evaluation and revealed that the MYH7-R723C and MLP-W4R mutations synergistically regulated sarcomere disorganization phenotype ($F(1,12)=12.25$, $p=0.0044$; each mutation considered as an independent factor). Data in the graph are presented as mean \pm S.E.M; $n=4$ independent cardiomyocyte differentiation batches; ** $p<0.01$; *** $p<0.001$; **** $p<0.0001$; N.S.: not significant. **L**, Quantification of *BNP* mRNA expression levels in day 35 control, MLP-W4R, MYH7-R723C and MLP-W4R;MYH7-R723C proband iPSC-CMs with qRT-PCR. Expression levels were normalized to *GAPDH* and fold change in relation to control was presented ($n=6$ independent cardiomyocyte differentiation batches). Two-way ANOVA with Tukey's multiple comparison test was used for statistical evaluation and revealed that the MYH7-R723C and MLP-W4R mutations synergistically upregulated *BNP* mRNA expression in the MLP-W4R;MYH7-R723C proband iPSC-CMs ($F(1,20)=6.670$, $p=0.0178$; each mutation considered as an independent factor). # denotes that proband iPSC-CMs exhibited significantly higher *BNP* expression levels than MLP-W4R ($p=0.0007$), MYH7-R723C ($p=0.0035$), or control ($p=0.0003$) iPSC-CMs. Note that the H value indicates Kruskal-Wallis H Test statistics and the degrees of freedom (df) represent the df for experimental groups (I). Additionally, F values indicate the ratio of explained variance between groups to unexplained variance due to experimental variations within groups, and df represent the df for factor interaction (two-way ANOVA) and the sum of the individual df for each experimental group (K and L). Each data point represents a single batch of iPSC-CMs (I, K, and L) from at least four independent cardiomyocyte differentiation batches. Data in the graph are presented as mean \pm S.E.M; * $p<0.05$.

Figure S2. CRISPR/Cas9-Mediated Correction of the Heterozygous MYH7-R723C Missense Mutation in MLP-W4R;MYH7-R723C Proband iPSCs. Related to Figure 2.

A, Overall strategy for CRISPR-mediated genetic correction of missense mutation in the target exon 20 of the *MYH7* gene is shown. gRNA sequence (minus strand, blue) with protospacer adjacent motif (PAM) sequence (green) is shown in the magnified inset. Point mutation (red; C to T in the bottom strand; also see panel D sequence) is located 78 bp downstream the PAM sequence. **B**, A DNA sequence of 901 bp strand was ligated into the pUC19 circular plasmid and supplied as template to facilitate homologous recombination at the target locus. Corrected base 'C' (red) was introduced into the construct. The neighboring BamHI restriction site (GGATCC, bold with underline) was introduced via a silent nucleotide change in the template DNA to facilitate subsequent screening of the corrected iPSC clones with successful homologous DNA recombination. The base 'C' of the PAM sequence was also replaced with the base 'T' as a silent change in the template DNA to avoid template DNA cutting or rebinding of the gRNA to the target sequence leading to Cas 9 recleavage after successful correction. **C**, Representative agarose gel showing the BamHI-mediated restriction digestion of the PCR product of the target DNA of a successfully corrected iPSC clone. **D**, Confirmation of successful correction of the mutant base to wild-type sequence in the corrected iPSC clone by Sanger sequencing. The BamHI restriction site is underlined. The red and green arrows point to the corrected and silent bases, respectively. **E**, Sequencing for the top 10 potential off-target genomic sites for the gRNA (see Table S4). Potential off-target genomic sites were computationally predicted using an online CRISPR Design Tool (<http://crispr.mit.edu/>) published by Ran *et al.*, Nature Protocol 2013, 8 (11): 2281-2308. Sanger sequencing of the predicted potential off-targets revealed no gRNA-mediated non-specific cleavage by Cas9. Potential off-target sequences are shaded in Sanger sequencing. **F**, Karyotyping of the MYH7-R723C corrected iPSCs. MYH7-R723C-corrected iPSC clone showed normal karyotypes.

Figure S3. TALEN-Mediated Correction of the Heterozygous MLP-W4R Missense Mutation in MLP-W4R;MYH7-R723C Proband iPSCs. Related to Figure 2.

A, Overall strategy for TALEN-mediated MLP-W4R gene correction in the exon 3 of the *CSRP3* (encoding MLP protein) gene is shown. Left and right TALEN DNA binding domains coupled with the FokI cleavage domain flank the point mutation (T to C; red). **B**, A 135 bp long MLP antisense single-stranded oligodeoxynucleotide (AS-ssODN) was supplied as a donor template to support homologous DNA directed recombination. The MfeI restriction site (CAATTG, underlined) was introduced via silent nucleotide change in the AS-ssODN to facilitate restriction digestion-based screening for gene-corrected iPSC clones after successful homologous DNA recombination. **C**, Representative agarose gel showing MfeI-mediated restriction digestion of the PCR amplicon of the target region in an MLP-W4R-corrected clone. **D**, Confirmation of reversion of the mutant base to wild-type sequence in the corrected iPSC clone by the Sanger sequencing. The red arrow in the top panel (MLP-W4R sequence) points to mutation (T to C). The red and green arrows in the bottom panel (MLP-W4R-corrected sequence) point to the corrected and silent change bases, respectively. The MfeI restriction site is underlined in the target genomic site. Genome-wide searching for the TALEN-targeted 54 nucleotide bases in the MLP gene with the Nucleotide BLAST program did not reveal existing, non-specific matching in the human genome. **E**, Karyotyping of the MLP-W4R corrected iPSCs. MLP-W4R-corrected iPSC clone showed normal karyotypes.

Figure S4. Measurement of Ca²⁺ Transients and Proteins Involved in Sarcoplasmic Reticulum Calcium Reuptake in iPSC-CMs. Related to Figure 3.

A, Representative traces of raw Ca²⁺ transients in day 35 control, MLP-W4R, MYH7-R723C, and MLP-W4R;MYH7-R723C iPSC-CMs paced at 1Hz. **B-C**, Quantification of systolic calcium intracellular release (**B**) and resting calcium levels during diastolic relaxation (**C**) in beating iPSC-CMs. **D**, Representative normalized Ca²⁺ transients in day 35 control, MLP-W4R, MYH7-R723C, and MLP-W4R;MYH7-R723C iPSC-CMs. Ca²⁺ transients for each cell type from panel A were normalized to their individual maximum and minimum. **E**, Measurement of Ca²⁺ transient decay (Tau80) in day 35 control, MLP-W4R, MYH7-R723C, and MLP-W4R;MYH7-R723C iPSC-CMs. **F**, A representative western blot image showing SERCA2a protein levels in day 35 control, MLP-W4R, MYH7-R723C, and MLP-W4R;MYH7-R723C iPSC-CMs. **G**, Quantification of SERCA2a protein

levels. GAPDH was used as a loading control. **H**, A representative western blot image showing phosphorylated phospholamban (P-PLB) and total PLB (T-PLB) protein levels in day 35 control, MLP-W4R, MYH7-R723C, and MLP-W4R;MYH7-R723C iPSC-CMs. **I**, Quantification of P-PLB and T-PLB protein levels. GAPDH was used as a loading control. Two-way ANOVA with Tukey's multiple comparisons test was used for statistical analyses and revealed that the MYH7-R723C mutation regulated systolic Ca^{2+} intracellular release (**B**, $F(1,434)=66.040$, $p<0.0001$), diastolic Ca^{2+} levels (**C**, $F(1,434)=81.660$, $p<0.0001$), Tau80 (**E**, $F(1,434)=32.380$, $p<0.0001$), SERCA2a protein levels (**G**, $F(1,24)=25.200$, $p<0.0001$), and the ratios of P-PLB to T-PLB (**I**, $F(1,20)=14.020$, $p=0.0013$), independent of the MLP-W4R mutation in iPSC-CMs. Note that F values indicate the ratio of explained variance between groups to unexplained variance due to experimental variations within groups, and the degrees of freedom (df) represent the df for each factor (genotype) and the sum of the individual df for each experimental group, respectively (B, C, E, G, and I). Each mutation is considered as an independent factor. Each data point represents a single iPSC-CM cluster (B, C, and E) or sample generated from a batch of iPSC-CMs (G and I) from at least three independent cardiomyocyte differentiation batches. All data in the graphs are presented as mean \pm S.E.M; ** $p<0.01$; **** $p<0.0001$.

Figure S5. Modulation of the HCM Phenotype in iPSC-CMs via Ectopic Expression of the Wild-Type MLP Protein, the Mutant MLP-W4R Protein, or Treatment of Mavacamten. Related to Figures 4 and 5.

A, cTnT and GFP immunostaining of day 35 control and MLP-W4R;MYH7-R723C iPSC-CMs infected with GFP or HA-tagged MLP-WT lentiviruses on days 21-22. DNA was counter stained by DAPI. Scale bar, 100 μm . **B**, Quantification of lentiviral infection intensities measured by cellular GFP pixels in control and MLP-W4R;MYH7-R723C iPSC-CMs. One-way ANOVA with Tukey's multiple comparisons test was used for statistical evaluation and revealed no difference in lentiviral infection intensity per iPSC-CM amongst the four different experimental groups ($F(3,1296)=2.408$, $p=0.066$). **C**, Quantification of percentage of control and MLP-W4R;MYH7-R723C iPSC-CMs infected by GFP or MLP-WT lentiviruses. ImageJ was used to measure GFP pixels (gray value). Kruskal-Wallis with Dunn's multiple comparisons test was used for statistical evaluation

and revealed no difference in percent of infected iPSC-CMs amongst the four different experimental groups ($H(3)=0.282$, $p=0.963$). **D**, cTnT and GFP immunostaining of day 35 control and MYH7-R723C iPSC-CMs infected by GFP or HA-tagged MLP-W4R lentiviruses on days 21-22. DNA was counter stained by DAPI. Scale bar, 100 μm . **E**, Quantification of lentiviral infection intensities measured by cellular GFP pixels in control and MYH7-R723C iPSC-CMs. One-way ANOVA with Tukey's multiple comparisons test was used for statistical evaluation and revealed no difference in lentiviral infection intensity per iPSC-CM amongst the four different experimental groups ($F(3,1213)=1.621$, $p=0.183$). **F**, Quantification of percentage of control and MYH7-R723C iPSC-CMs infected by GFP or MLP-W4R lentiviruses. Kruskal-Wallis with Dunn's multiple comparisons test was used for statistical evaluation and revealed no difference in percent of infected iPSC-CMs amongst the four different experimental groups ($H(3)=0.728$, $p=0.890$). **G**, cTnT and GFP immunostaining of day 35 MYH7-R663H iPSC-CMs infected by GFP or HA-tagged MLP-W4R lentiviruses on days 21-22. Scale bar, 100 μm . **H**, Quantification of lentiviral infection intensities measured by cellular GFP pixels in MYH7-R663H iPSC-CMs. A two-tailed unpaired Student's t test was used for statistical evaluation and revealed no difference in lentiviral infection intensity per iPSC-CM between the two groups. **I**, Quantification of percentage of MYH7-R663H iPSC-CMs infected by GFP or MLP-W4R lentiviruses. A two-tailed unpaired Mann-Whitney U test was used for statistical evaluation and revealed no difference in percent of infected iPSC-CMs between the two groups. **J**, cTnT and GFP immunostaining of day 35 MYH7-R442G iPSC-CMs infected by GFP or HA-tagged MLP-W4R lentiviruses on days 21-22. Scale bar, 100 μm . **K**, Quantification of lentiviral infection intensities measured by cellular GFP pixels in MYH7-R442G iPSC-CMs. A two-tailed unpaired Student's t test was used for statistical evaluation and revealed no difference in lentiviral infection intensity per iPSC-CM between the two groups. **L**, Quantification of percentage of MYH7-R442G iPSC-CMs infected by GFP or MLP-W4R lentiviruses. A two-tailed unpaired Mann-Whitney U test was used for statistical evaluation and revealed no difference in percent of infected iPSC-CMs between the two groups. **M**, cTnT and GFP immunostaining of day 35 MYBPC3-R943x iPSC-CMs infected by GFP or HA-tagged MLP-W4R lentiviruses on days 21-22. Scale bar, 100 μm . **N**, Quantification of lentiviral infection intensities measured by cellular

GFP pixels in MYBPC3-R943x iPSC-CMs. A two-tailed unpaired Student's t test was used for statistical evaluation and revealed no difference in lentiviral infection intensity per iPSC-CM between the two groups. **O**, Quantification of percentage of MYBPC3-R943x iPSC-CMs infected by GFP or MLP-W4R lentiviruses. A two-tailed unpaired Mann-Whitney U test was used for statistical evaluation and revealed no difference in percent of infected iPSC-CMs between the two groups. **P**, cTnT and GFP immunostaining of day 35 MYBPC3-V321M iPSC-CMs infected by GFP or HA-tagged MLP-W4R lentiviruses on days 21-22. Scale bar, 100 μ m. **Q**, Quantification of lentiviral infection intensities measured by cellular GFP pixels in MYBPC3-V321M iPSC-CMs. A two-tailed unpaired Student's t test was used for statistical evaluation and revealed no difference in lentiviral infection intensity per iPSC-CM between the two groups. **R**, Quantification of percentage of MYBPC3-V321M iPSC-CMs infected by GFP or MLP-W4R lentiviruses. A two-tailed unpaired Mann-Whitney U test was used for statistical evaluation and revealed no difference in percent of infected iPSC-CMs between the two groups. **S**, Schematic of the NFAT-luciferase reporter. Nine copies of an NFAT binding site from the *IL-4* promoter were placed 5' to a minimal promoter of the α -myosin heavy chain gene (-164 to +12) and introduced upstream of the luciferase reporter in pGL-3 Basic plasmid to generate the NFAT-luciferase reporter⁴⁹. **T**, Measurement of normalized NFAT-luciferase activity in control and proband MLP-W4R;MYH7-R723C iPSC-CMs. Cardiomyocytes were transiently transfected at day 25 of cardiac differentiation with NFAT-luciferase reporter (9xNFAT-luciferase) and Renilla-luciferase (pLX313 from Addgene) that is driven by the constitutively active EF-1 α promoter⁵⁰ and works as an internal transfection control. Luciferase activities were measured two days after transfection using the Dual-Glow kit (Promega). NFAT-luciferase activities were normalized by Renilla-luciferase, and fold change was calculated in relation to control CMs. A two-tailed unpaired Mann-Whitney U test was used to evaluate statistical difference. **U-W**, Dosage effects of mavacamten in rescuing HCM defects in proband iPSC-CMs. **U**, *BNP* mRNA expression levels in MLP-W4R;MYH7-R723C iPSC-CMs treated with either vehicle control (DMSO) or different doses (0.1, 0.3, 0.5, and 1.0 μ M) of mavacamten. Treatment was started on day 25 of cardiac differentiation. *BNP* expression levels were analyzed 24 hours after drug treatment using qRT-PCR and normalized to the housekeeping gene *GAPDH*.

Kruskal–Wallis with Dunn’s multiple comparisons test was performed for *BNP* expression ($H(4)=16.060$, $p=0.0029$). **V**, Immunostaining of cTnT (green) in MLP-W4R;MYH7-R723C iPSC-CMs treated with either vehicle control or mavacamten at different doses for 4 days. Scale bar, 100 μm . **W**, Cell areas were quantified in vehicle or mavacamten-treated MLP-W4R;MYH7-R723C iPSC-CMs. One-way ANOVA with Tukey’s multiple comparison test was performed for cell area differences ($F(4,2380)=124.700$, $p<0.0001$). Image J was used to quantify of iPSC-CM area in panel V from five independent cardiomyocyte differentiation batches (≥ 50 cells per batch for each dose). Note that mavacamten at 0.5 μM was selected for subsequent experiments based on the significant effect of mavacamten at 0.5 μM in reducing both elevated expression of *BNP* and enlarged cell area in proband CMs. **X-Z**, mRNA expression levels of three known HCM marker genes *ACTA1* (skeletal α -actin, **X**), *ANF* (atrial natriuretic factor, **Y**), and *ANKRD1* (cardiac ankyrin repeat protein [CARP], **Z**) were measured in vehicle control (DMSO)- or 0.5 μM mavacamten-treated proband iPSC-CMs. Cardiomyocytes were treated at day 25 of cardiac differentiation for 24 hours. A two-tailed unpaired Mann-Whitney U test was used for gene analysis. mRNA expression levels were normalized to the *GAPDH* gene. **Y’**, Quantification of *MCIP1* gene expression levels in mavacamten treated MLP-W4R;MYH7-R723C proband iPSC-CMs. Day 25 MLP-W4R;MYH7-R723C iPSC-CMs were treated with DMSO vehicle control or 0.5 μM mavacamten for 24 hours, followed by qRT-PCR quantification of *MCIP1* mRNA expression. Gene expression levels were normalized to *GAPDH* and fold change relative to vehicle treated group was presented. **Z’**, Measurement of normalized NFAT-luciferase activity in vehicle (DMSO) and mavacamten-treated (0.5 μM) MLP-W4R;MYH7-R723C iPSC-CMs. Cardiomyocytes were treated with DMSO or mavacamten on day 25 of cardiac differentiation, transiently transfected with NFAT-luciferase reporter and Renilla-luciferase on day 27 for 6 hours, and luciferase activities measured on day 29. A two-tailed unpaired Mann-Whitney U test was used for statistical evaluation between vehicle and mavacamten treated groups (**X-Z’**). Note that F values indicate the ratio of explained variance between groups to unexplained variance due to experimental variations within groups, and the degrees of freedom (df) represent the df for experimental groups and the sum of the individual df for each experimental group, respectively (B, E, and W). Additionally, H values indicate

Kruskal Wallis H Test statistics and df represent the df for experimental groups (C, F, and U). Each data point represents a single iPSC-CM (B, E, H, K, N, Q, and W) or sample generated from a batch of iPSC-CMs (C, F, I, L, O, R, T, U, X, Y, Z, Y', and Z') from at least three independent cardiomyocyte differentiation batches. All data in the graphs are presented as mean \pm S.E.M; *p<0.05; **p<0.01; ***p<0.001; ****p<0.0001; N.S.: not significant.

Supplemental Videos Legends

Video S1. Echocardiogram video of the proband (MLP-W4R_MYH7-R723C)

Video S2. Echocardiogram video of the proband's mother (MLP-W4R)

Video S3. Echocardiogram video of the proband's father (MYH7-R723C)